Journal of ELECTRONIC MATERIALS, Vol. 41, No. 4, 2012
DOI: 10.1007/s11664-012-1932-x

Surface Morphology of Sn-Rich Solder Interconnects After Electrical Loading

Q.S. ZHU,[1,3] H.Y. LIU,[1] Z.G. WANG,[1] and J.K. SHANG[1,2]

1.—Shenyang National Laboratory for Materials Science, Institute of Metal Research, Chinese Academy of Sciences, Shenyang 110016, China. 2.—Department of Materials Science and Engineering, University of Illinois at Urbana-Champaign, Urbana, IL 61801, USA. 3.—e-mail: qszhu@imr.ac.cn

Morphological changes from electromigration were examined on microsized Sn-Ag-Cu, pure Sn, and single-crystal Sn solder interconnects. It was found that both grain structure and alloying had a strong influence on the form of electromigration damage. In polycrystal Sn, grain boundary grooves were the primary form of electromigration damage, while in single-crystal Sn interconnects wavy surface relief appeared following electromigration. Alloying with Ag and Cu encouraged formation of Sn hillocks and Cu_6Sn_5 intermetallic compound (IMC) segregation. The grain boundary grooves were related to the divergence of the vacancy concentration at grain boundaries, which induced Sn grain tilting or sliding. Removal of the grain boundaries in the single-crystal interconnect made surface diffusion the primary electromigration mechanism, resulting in wavy surface relief after long electromigration time. In Sn-Ag-Cu alloy, directional flow of Cu caused Cu_6Sn_5 IMC segregation, which produced large compressive stress, driving the stressed grains to grow into hillocks.

Key words: Solder interconnect, electromigration, hillock, grain boundary groove

INTRODUCTION

Solder interconnects have been used to provide both electrical and mechanical connections in packaging of various microelectronic devices. Recent studies on electric loading of solder interconnects found that Pb-free solders were susceptible to electromigration.[1–3] The electromigration led to formation of voids and hillocks, segregation of elements, and growth or dissolution of the intermetallic compounds (IMCs) at the electrodes. The solder interconnects exhibited reduced strength[4] and elevated stress relaxation or creep rate.[5,6] In some extreme cases, the electric current even induced brittle fracture of the interconnect near the cathode.[7,8] It is therefore imperative to understand electromigration in Pb-free solder interconnects.

(Received August 3, 2011; accepted January 12, 2012; published online February 17, 2012)

Electromigration is known to be a directional diffusion process, where atoms and vacancies are driven by the electron wind force. The alloying elements in Sn-based solder usually have different atomic diffusivities compared with Sn. In the case of Sn-based solder with similar diffusivity to Sn, such as eutectic Sn-Pb and Sn-Bi, phase separation is often observed after electromigration testing.[9,10] For eutectic Sn-Ag-Cu solder interconnects, in which the alloying elements are in low concentration, the migrations of Ag and Cu are insignificant as compared with that of Sn. Instead, fast interstitial diffusion of Cu, Ni, and Ag induces dissolution of under bump metallurgy (UBM) and IMC. Subsequently, the polarity effect of the interfacial IMC is predominant rather than phase separation.[11,12] In addition to atomic migration from cathode to anode, a recent study[4] on a microsized Sn-Ag-Cu interconnect showed that Sn hillocks appeared on the surface, suggesting that the atomic diffusion path is perpendicular to the current direction. The surface

morphology of solder interconnects may therefore be used as a monitor to understand the atomic diffusion mechanism during electromigration.

In this study, the surface morphologies of microsized Sn-3.5Ag-0.7Cu, pure Sn, and single-crystal Sn solder interconnects were examined post electromigration testing. The goal was to examine the effect of microstructure on the electromigration behavior of Pb-free solders. A mechanism based on vacancy and atom diffusion was established to explain well the difference in surface morphologies among the Sn-3.5Ag-0.7Cu, pure Sn, and single-crystal Sn solder interconnects.

EXPERIMENTAL PROCEDURES

The Sn-Ag-Cu and pure Sn solder interconnects in this study were made by reflow soldering using Sn-3.8Ag-0.7Cu solder and pure Sn. Copper cubes were ground and carefully polished to obtain clean surfaces before soldering flux was applied. For the Sn-Ag-Cu interconnect, copper wires were placed between two adjacent surfaces 300 μm apart to achieve a controlled solder joint thickness. For the pure Sn interconnect, a molybdenum wire was used to control the solder thickness, as shown in Fig. 1a. After the two cubes were aligned and fixed, the assembly was heated in an oven filled with N_2, where the solder was reflowed at 250°C for 40 s.

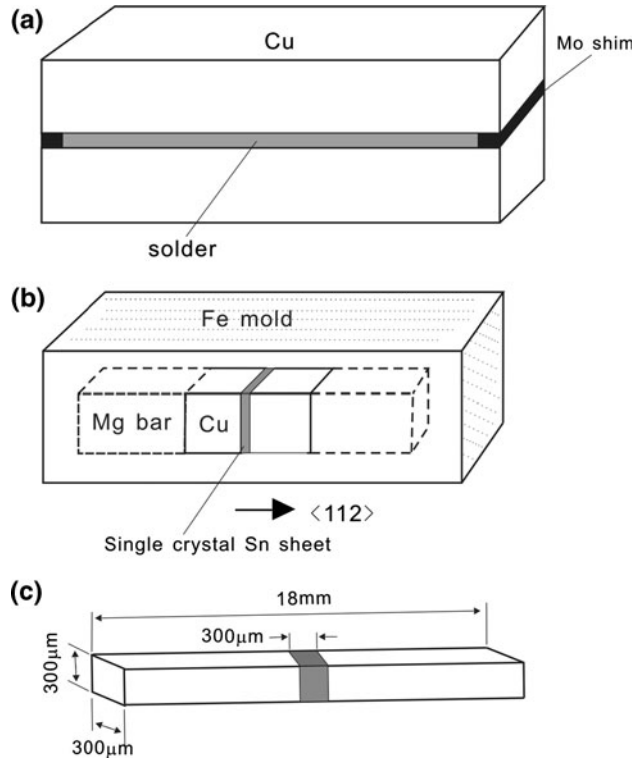

Fig. 1. Schematic diagrams of: (a) sample preparation of Sn-Ag-Cu and pure Sn solder interconnects, (b) sample preparation for single-crystal Sn interconnects, and (c) size of finished samples.

The single-crystal Sn plate was grown from 99.999% purity Sn balls using the Bridgman method in a horizontal furnace. The Sn plate was first cut into numerous thin sheets vertically along the growth direction using electric discharge machining. These sheets were then thinned to thickness of 300 μm using mechanical polishing. The crystalline orientation of these thin sheets was determined to be $\langle 112 \rangle$ by the x-ray diffraction (XRD) method. A thin sheet was sandwiched by two Cu bars, later being mounted into a steel mold in which two Mg bars were used as mandrills. Since the thermal expansion coefficient of Mg is higher than that of iron, compressive stress may be generated along the direction of the Cu bar when the mold is heated above ambient temperature. Figure 1b illustrates the sample preparation details. The mold was then placed into a vacuum furnace where the pressure was pumped to 10^{-3} Pa and the temperature was controlled to be 130°C, which is much lower than the melting point (232°C) of pure tin. After the thermocompression process, single-crystal Sn interconnects were achieved. The bulk solder joints of Sn-Ag-Cu, pure Sn, and single-crystal Sn were cut into samples by electric discharge machining. The cross-section of the samples was 300 μm × 300 μm, as shown in Fig. 1c.

These microsized solder interconnect samples were thoroughly polished to a mirror-like surface prior to electromigration testing. A constant direct current with density of 3×10^4 A/cm^2 was applied to the solder interconnect sample. All samples were immersed in a heat-conducting oil during the electromigration test to minimize surface oxidation and to dissipate Joule heating, as shown in Fig. 2. Selected samples were removed from the oil bath at different stages of the electromigration test, then cleaned and examined by scanning electron microscopy (SEM).

RESULTS

After the electromigration test for 150 h, the surface of the Sn-Ag-Cu solder interconnect became fairly rough, as shown in Fig. 3a, b. Surface protuberances appeared with different shapes and sizes.

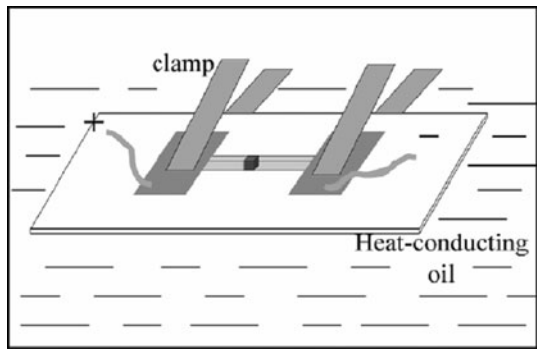

Fig. 2. Schematic diagram of electromigration test.

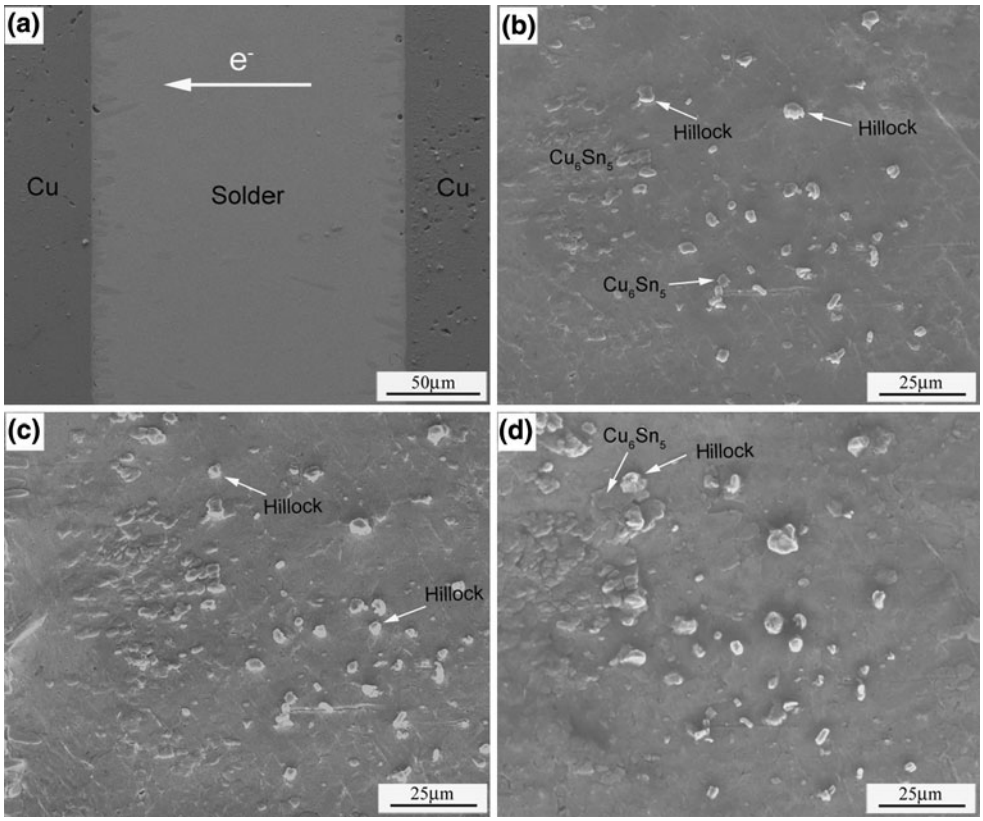

Fig. 3. Surface morphology of the Sn-Ag-Cu solder interconnect: (a) before electromigration, (b) after electromigration for 150 h, (c) after electromigration for 190 h, and (d) after electromigration for 250 h.

EDS analysis suggested that the composition for the relatively higher and brighter protuberances was pure tin. These protuberances were identified as Sn hillocks. Accordingly, the protuberances which appeared to be relatively lower and darker were identified to be Cu_6Sn_5 IMCs. *In situ* observation found that the Sn hillocks grew and coarsened significantly with increasing testing time, as shown in Fig. 3b–d. The surface roughness appeared to be closely related to the intergrowth of Sn hillocks and Cu_6Sn_5 IMC during the electromigration test. Electron probe microanalysis (EPMA) indicated that the center area contained negligible Cu signals in the post electromigration test samples. However, the sample surface area had much higher Cu concentration, indicating surface segregation of Cu atoms. The Cu segregation was represented mostly by Cu_6Sn_5 IMC, which was clearly distinguishable from the Sn hillocks by changing the SEM image mode from secondary electron (SE) to backscattered diffraction (BSD), as shown in Fig. 4. The current-induced Sn hillock was similar to that found in the electrodeposited pure Sn layer.[13]

Sn hillocks and Cu_6Sn_5 IMCs were rarely observed in pure Sn interconnects after the electromigration test, as shown in Fig. 5a, b. Instead, the surface morphology was characterized by grain boundary grooves. The formation of these grain boundary grooves is due to motion of grain boundaries, i.e., tilting or rotation. Grain rotation resulting from electromigration was reported in Sn solder interconnects previously,[6] where one side of the grain rose while the other side sank, as shown in Fig. 5c. After extending the electromigration test, the grain boundary grooves deepened because the grain continued to rotate under the electric current, as shown in Fig. 5d. A similar surface grooving phenomenon was also reported elsewhere on pure Sn stripe after electromigration.[14] Different from the Sn hillock, the grain boundary groove does not change the original grain in terms of its shape or size.

During the electromigration test, Cu atoms diffuse from the Cu metallization at the cathode to the anode under the direct current. Although the surface diffusivity is much larger than the lattice and grain boundary diffusion coefficient, Cu segregation from the substrate was seldom observed on the surface of the pure Sn interconnect after the electromigration test. This suggested that Cu segregation on the Sn-3.5Ag-0.7Cu surface was due to Cu sourced from inside the solder rather than from the Cu substrate at the electrode.

When the single-crystal Sn interconnects were subjected to the same current stressing, the surface remained smooth for a fairly long time, as shown in

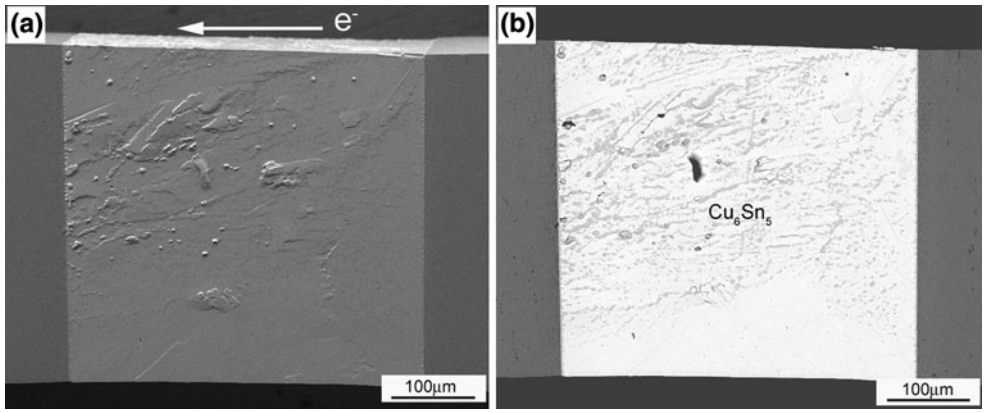

Fig. 4. Hillock growth and Cu_6Sn_5 IMC phase segregation on the surface after electromigration: (a) SEM in SE mode, (b) SEM in BSD mode.

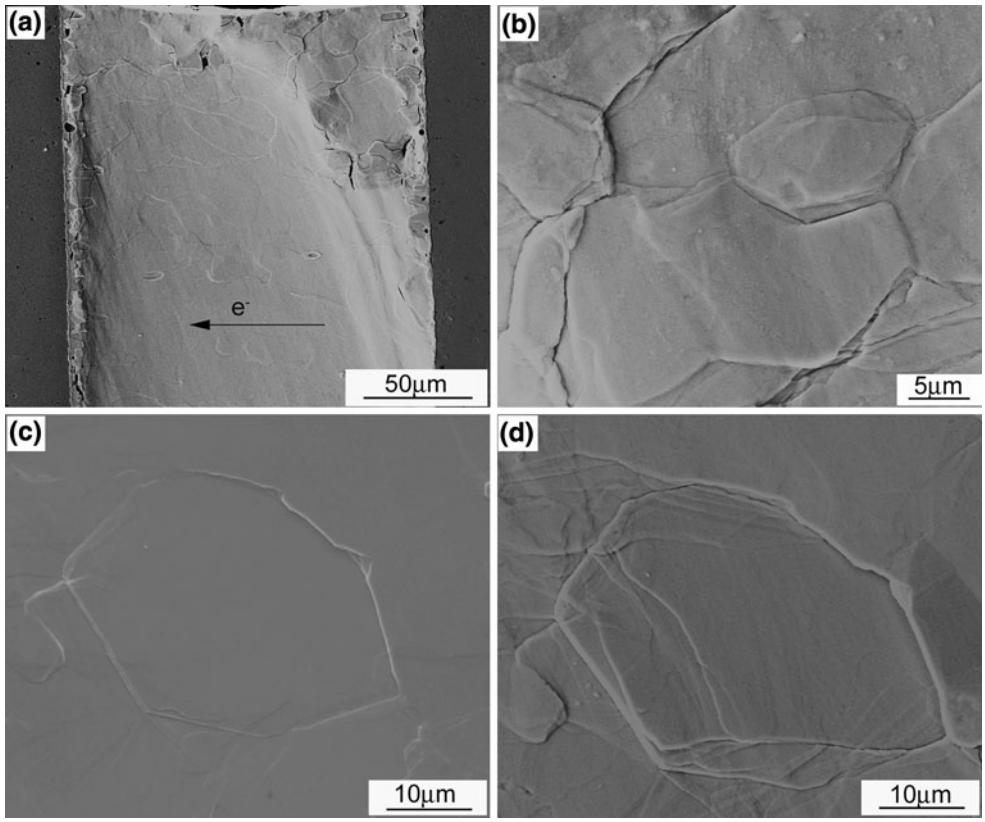

Fig. 5. Surface morphology of the pure Sn interconnect: (a) after electromigration for 180 h, (b) magnified image of grain boundary groove morphology, (c) grain rotation after electromigration for 130 h, and (d) further grain rotation after electromigration for 180 h.

Fig. 6a. It must be noted here that mark A is a polishing-induced defect. After the electromigration test, a wave-like relief traversed the surface and the relief became wider with increasing electromigration time, as shown in Fig. 6b, c. Observations from multiple samples suggested that the location of the wave-like relief was random. These features indicated that the formation of the wave-like relief may be related to surface diffusion driven by the electric current with a nonuniform density distribution on the surface.

DISCUSSION

Electromigration is often defined as directional flow of metal atoms under an electric field. For common metals, the driving force for electromigration comes from the impinging of electrons on atoms. As a result, the atoms move from the cathode to the anode with an electron flux. Accordingly, a flux of vacancies diffuses in the opposite direction. Usually, the vacancies accumulate to a certain concentration to form voids at the cathode side. On the other hand, the pile-up of atoms is accommodated

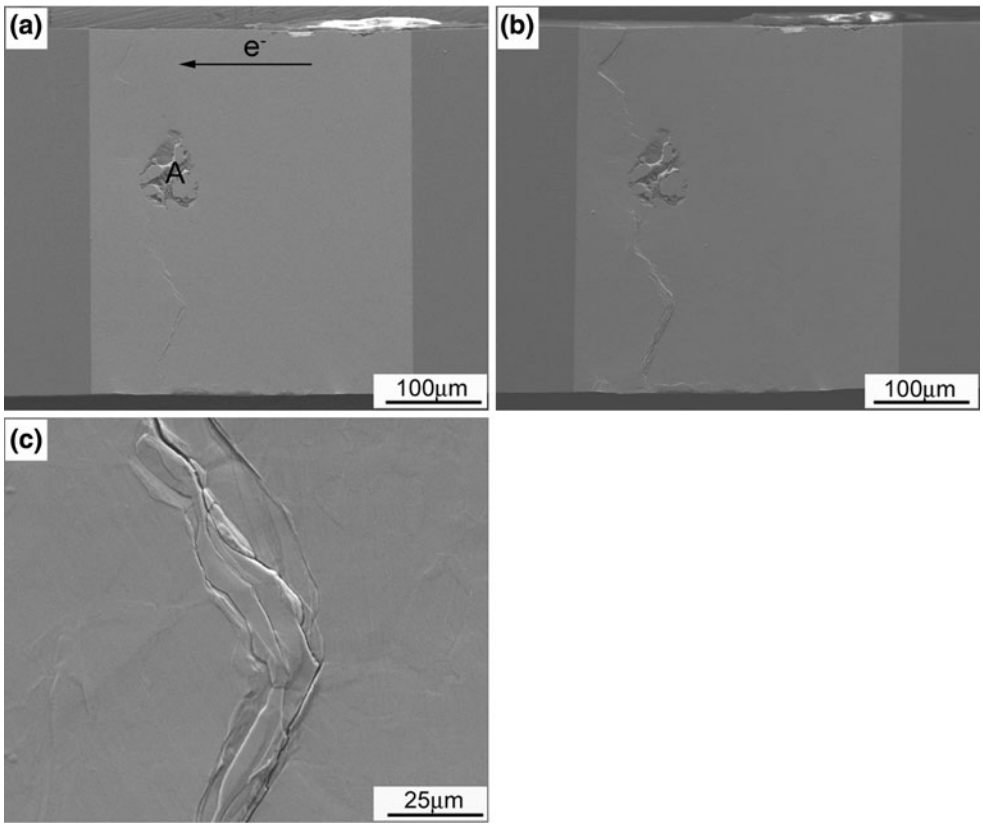

Fig. 6. Surface morphology of the single-crystal Sn interconnects: (a) after electromigration for 130 h, (b) after electromigration for 250 h, and (c) magnified image of the relief.

through volume expansion of interfacial intermetallic compound at the anode side.[11,12,14]

It is well known that grain boundaries are primary diffusion channels for Cu atomic transport during electromigration testing because the diffusivity of atoms through a grain boundary is about 10^6 times faster than that inside the lattice at room temperature. Figure 7 illustrates the formation of mechanical stress at trigeminal grain boundaries under the driving force of the electron wind. When the number of atoms flowing out of a trigeminal grain boundary is greater than those flowing in, a concentration gradient of vacancies is created. Tensile stress is built up accordingly at this trigeminal grain boundary. Similarly, when the number of atoms flowing into the trigeminal grain boundary is greater than those transported out, the excess atoms create compressive stress locally. Under the current experimental condition, the stress can be a function of the vacancy concentration as described below,[15]

$$\sigma = \frac{kT}{\Omega}\frac{\Delta C_V}{C_V^0},$$

where Ω is the atomic volume, k is the Boltzmann constant, T is the temperature, ΔC_V is the vacancy concentration, and C_V^0 is the initial vacancy concentration. The above equation predicts that the amount of stress increases with increasing vacancy concentration at the grain boundary.

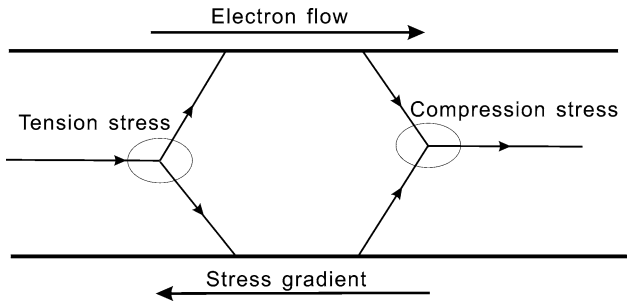

Fig. 7. Schematic diagram of stress generation at a trigeminal grain boundary by electromigration.

When there is a divergence of the vacancy concentration at the grain boundaries, this divergence could generate a torque. This torque, imposed on one grain, especially a surface free grain, can rotate the grain. The grain rotation phenomena had been directly observed in previous study where Sn strips were used in the electromigration test.[15] It was also reported that the rotated grain had a crystalline orientation favorable to electric resistance.[16] On the other hand, the stress at the grain boundary during electromigration can also promote Coble creep, in which atoms move along grain boundaries onto the

surfaces. This then results in grain boundary sliding to accommodate the diffusional flow. Because of the occurrence of grain rotation or sliding, grain boundary grooves appeared on the surface of the pure Sn interconnects after electromigration. With increasing electromigration time, the vacancy concentration at grain boundaries elevated so that both stress and torque were accelerated. Accordingly, the depth of the grain boundary grooves increased with extended electromigration test.

In this study, the solder interconnect samples were immersed in a heat-conducting oil to dissipate Joule heating. The temperature of the heat-conducting oil near the sample surface was measured to be within the range of 60°C to 70°C. Using the temperature value measured on the electromigration sample tested in air as a reference, the temperature of the center of the interconnect was estimated to be higher by 100°C. A thermal gradient above 1000°C/cm was created between the sample center and surface, which was sufficient to induce thermomigration according to previous studies.[17,18] Under the condition of thermomigration, Cu atoms had a tendency to move to the cold end. When the Cu atoms migrated from the center area onto the surface with the lowest energy state, segregation of Cu_6Sn_5 IMC occurred on the surface.

The equilibrium solubility of Cu in solid Sn is very small, i.e., 6×10^{-3} mass fraction Cu at 227°C and 10^{-7} mass fraction Cu at room temperature.[13] Cu diffusion in the Sn lattice is extremely fast, especially when driven by a large thermal gradient. It may be assumed that Cu is dissolved interstitially in Sn.[19] When Cu_6Sn_5 precipitated from a saturated Sn(Cu) solid solution, there was a difference between the molar volume of the saturated solution and the volume of an equilibrium mixture of Sn and Cu_6Sn_5 with the same composition. The volume of the saturated solution expanded when transformed into the equilibrium phases of Cu_6Sn_5 and Sn. Thus, the volume strain would create an in-plane compressive stress near the surface grain layer.

Similar to the growth of Sn whiskers, hillock growth is often treated as localized diffusional creep and/or grain boundary sliding that relieves compressive stress.[13] For Sn-rich solders with low melting temperature, grain boundary diffusion is expected to be the predominant self-diffusion mechanism. In-plane compressive stress is assumed to drive the flux of Sn towards the hillock or whisker. Tu et al.[20] proposed a model for whisker or hillock growth based on an imposed constant in-plane compressive stress and grain boundary diffusion to the base of the hillock or whisker. Based on this model, hillock growth was strongly dependent on the compressive stress.

As shown in Fig. 8, it was noted that the hillock appeared to have a small flat top at its center, indicating the original location of the hillock grain prior to migration of its boundaries. For the pure Sn interconnects, under the low-level stress at the grain boundary, the surface grains can only tilt or slide slightly but

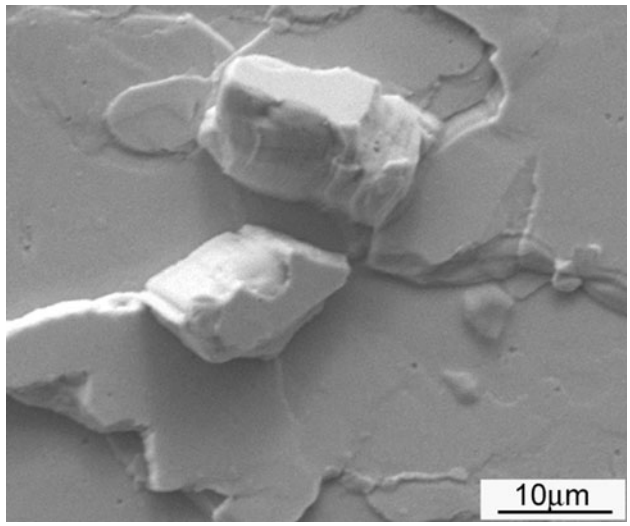

Fig. 8. Sn hillocks with a flat top during electromigration.

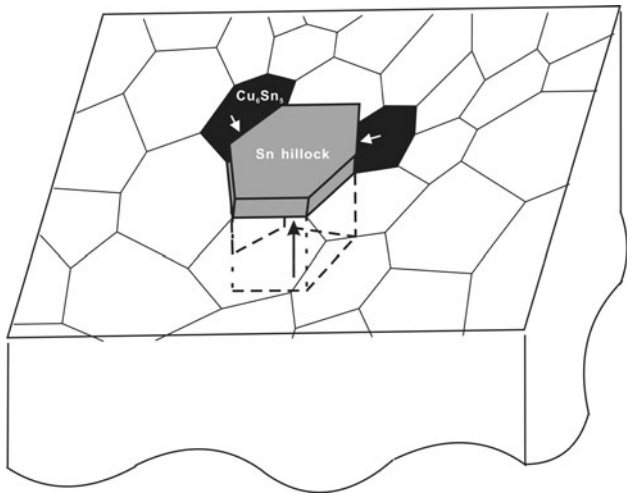

Fig. 9. Schematic diagram of Sn hillock growth under in-plane compressive stress from Cu_6Sn_5 segregation.

cannot grow into hillocks for lack of large compressive stress. In contrast, for the Sn-3.5Ag-0.7Cu solder interconnect, as drawn in Fig. 9, when a sufficient compressive stress was provided by the volume strain, the stressed grains would grow into hillocks. The hillocks grew larger with increasing electromigration time. The *in situ* observation also revealed that the hillocks grew at a faster rate initially when Cu_6Sn_5 segregation first started. The growth rate slowed down with the reduction in Cu_6Sn_5 segregation.

Since the formation mechanism of the grain boundary groove and hillock was related to the grain boundary, these surface features were not observed on the surface of single-crystal Sn solder. On the other hand, the surface diffusion of Sn under the electron wind force created a wave-like relief, which could be covered up by the other surface morphologies of pure Sn and Sn-Ag-Cu intercon-

nects but exposed on the single-crystal solder surface after electromigration.

CONCLUSIONS

1. After electromigration, grain boundary grooves appeared on the surface of pure Sn solder interconnects, while Sn hillocks and Cu_6Sn_5 IMC segregation appeared on the surface of Sn-3.5Ag-0.7Cu interconnects.
2. The surface of single-crystal Sn interconnects was relatively smooth initially, then appeared to have a wave-like relief morphology after long electromigration testing.
3. The grain boundary groove of the pure Sn interconnect, which resulted from grain tilting or sliding, was due to divergence of the vacancy concentration and Coble creep at the grain boundaries. The occurrence of the wave-like relief morphology on the single-crystal Sn interconnects was related to surface diffusion of Sn.
4. Cu_6Sn_5 IMC segregation on the surface of Sn-Ag-Cu solder generated a large in-plane compressive stress within the surface grain layers, which supported the stressed grains to grow further into hillocks.

ACKNOWLEDGEMENT

This study was financially supported by the National Basic Research Program of China, under Grant No. 2010CB631006, and the National Natural Science Foundation of China (NSFC), under Grant No. 51101161.

REFERENCES

1. K. Zeng and K.N. Tu, *Mater. Sci. Eng. R.* 38, 55 (2002).
2. K.N. Tu, *J. Appl. Phys.* 94, 5451 (2003).
3. Y.C. Chan and D. Yang, *Prog. Mater. Sci.* 55, 428 (2010).
4. L. Zhang, Z.G. Wang, and J.K. Shang, *Scripta Mater.* 56, 381 (2007).
5. H.Y. Liu, Q.S. Zhu, L. Zhang, Z.G. Wang, and J.K. Shang, *J. Mater. Res.* 5, 1172 (2010).
6. H.Y. Liu, Q.S. Zhu, Z.G. Wang, and J.K. Shang, *Mater. Sci. Eng. A* 528, 1467 (2011).
7. F. Ren, J.W. Nah, K.N. Tu, B.S. Xiong, L.H. Xu, and H.L. Pang, *Appl. Phys. Lett.* 89, 141914 (2006).
8. X.J. Wang, Q.S. Zhu, Z.G. Wang, and J.K. Shang, *J. Mater. Sci. Technol.* 26, 737 (2010).
9. S. Branderburg and S. Yeh, *Proceeding of Surface Mount International Conference and Exposition*, San Jose, CA (1998).
10. Q.L. Yang and J.K. Shang, *J. Electron. Mater.* 34, 1363 (2005).
11. Y.C. Hu, Y.H. Lin, C.R. Kao, and K.N. Tu, *J. Mater. Res.* 18, 2544 (2003).
12. Y.H. Lin, Y.C. Hu, C.R. Kao, and K.N. Tu, *Acta Mater.* 53, 2029 (2005).
13. W.J. Boettinger, C.E. Johnson, L.A. Bendersky, K.W. Moon, M.E. Williams, and G.R. Stafford, *Acta Mater.* 53, 5033 (2005).
14. H. Gan and K.N. Tu, *J. Appl. Phys.* 97, 063514 (2005).
15. A.T. Wu and T.C. Hsieh, *Appl. Phys. Lett.* 92, 121921 (2008).
16. A.T. Wu, K.N. Tu, J.R. Lloyd, N. Tamura, B.C. Valek, and C.R. Kao, *Appl. Phys. Lett.* 85, 2490 (2004).
17. H.Y. Hsiao and C. Chen, *Appl. Phys. Lett.* 90, 152105 (2007).
18. A.T. Huang, A.M. Gusak, K.N. Tu, and Y.S. Lai, *Appl. Phys. Lett.* 88, 141911 (2006).
19. B.F. Dyson, T.R. Anthony, and D. Turnbull, *J. Appl. Phys.* 38, 3408 (1967).
20. K.N. Tu, *Phys. Rev. B-Condens. Matter* 49, 2030 (1994).